

# Defining Operational Conditions for Safety-Critical AI-Based Systems from Data

Johann Maximilian Christensen<sup>1</sup> Elena Hoemann<sup>1</sup> Frank Köster<sup>1</sup> Sven Hallerbach<sup>1</sup>

## Abstract

Artificial Intelligence (AI) has been on the rise in many domains, including numerous safety-critical applications. However, for complex systems found in the real world, or when data already exist, defining the underlying environmental conditions is extremely challenging. This often results in an incomplete description of the environment in which the AI-based system must operate. Nevertheless, this description, called the Operational Design Domain (ODD), is required in many domains for the certification of AI-based systems. Traditionally, the ODD is created in the early stages of the development process, drawing on sophisticated expert knowledge and related standards. This paper presents a novel Safety-by-Design method to *a posteriori* define the ODD from previously collected data using a multi-dimensional kernel-based representation. This approach is validated through both Monte Carlo methods and a real-world aviation use case for a future safety-critical collision-avoidance system. Moreover, by defining under what conditions two ODDs are equal, the paper shows that the data-driven ODD can equal the original, underlying hidden ODD of the data. Utilizing the novel, Safe-by-Design kernel-based ODD enables future certification of data-driven, safety-critical AI-based systems.

## 1. Introduction

The rapid adoption of Artificial Intelligence (AI) across a wide range of application domains has fundamentally changed how complex systems are designed and operated. In safety-critical domains such as aviation, automotive systems, and industrial automation, AI-based components are increasingly responsible for perception, decision-making, and control (Bello et al., 2024; Stefani et al., 2024b). While

these capabilities enable unprecedented levels of autonomy and performance, they also introduce new challenges for safety assurance, validation, and certification. As a consequence, research into the safety of AI-based systems has only recently begun to catch up with their practical deployment. Especially in domains with stringent safety requirements, safety considerations are not merely desirable but mandatory to enable certification and operational approval (Mamalet et al., 2021; Rabe et al., 2021; Christensen et al., 2025). Current approaches to ensuring the safety of AI-based systems predominantly rely on reactive measures, such as extensive testing, runtime monitoring, and post hoc failure analysis. Although effective, these approaches are often time-consuming, costly, and difficult to scale. In contrast, Safety-by-Design methodologies aim to integrate safety considerations directly into the system development process, providing proactive guarantees rather than reactive mitigation.

This paradigm shift has given rise to the research field of AI Engineering, which seeks systematic, certifiable methods for designing AI-based systems from the outset. A central concept in Safety-by-Design AI Engineering is the Operational Design Domain (ODD) (Werner et al., 2025). The ODD specifies the set of operational conditions under which an AI-based system is intended to function safely. By explicitly defining these conditions, the ODD provides a foundation for system design and verification, and has become a key instrument in multiple regulatory frameworks. However, despite its importance, defining an ODD remains challenging. Traditionally, ODDs are created manually by domain experts early in the development process (Stefani et al., 2023). While expert-defined ODDs are effective when system behavior and environmental conditions are well understood, they become increasingly difficult to construct for complex real-world systems. These challenges motivate the need for data-driven approaches to ODD construction. Data-driven ODDs promise several advantages: they can capture complex, implicit parameter dependencies; naturally reflect real operational conditions; and are updated as new data become available.

This work addresses this gap by introducing a deterministic, kernel-based framework for data-driven ODD construction. Instead of manually creating an ODD and iteratively optimizing it, the proposed method constructs the ODD directly

<sup>1</sup>Institute for AI Safety and Security, German Aerospace Center (DLR), Sankt Augustin, Germany. Correspondence to: Johann Maximilian Christensen <johann.christensen@dlr.de>.

from data using samples as anchor points for analytically defined kernel functions. The resulting ODD representation is continuous, bounded, order-independent, and uniquely determined by the available data. Importantly, the method remains applicable even in sparse-data regimes, making it suitable for both early development stages and mature systems.

The aim of this work is to provide a mathematically rigorous, certifiable framework for deriving ODDs solely from data, while explicitly adhering to Safety-by-Design requirements. This work formalizes ODDs as mathematical structures, introduces a kernel-based affinity representation, and proposes an automated procedure for parameter selection and handling of out-of-distribution samples. By construction, the resulting ODD representation is deterministic and interpretable, enabling its use not only for modeling and monitoring but also as a foundation for future certification of AI-based systems.

The work is structured as follows: in Section 2, the current state of the art regarding ODDs and general Safety-by-Design AI Engineering methodologies is presented. Afterwards, in Section 3.1, a comprehensive framework for mathematically representing ODDs is defined. Next, Section 4 discusses the main contribution of this paper: a kernel-based, data-driven method to define ODDs purely from data, applicable also to use cases with only sparse data. The method is then validated throughout Section 5. Finally, in Section 6, the results are discussed, and in Section 7, the paper is concluded.

## 2. State of the Art

In the past, the concept of the Operational Design Domain found approval in both the automotive and aviation domains, with more currently following (Huseynzade, 2023; Adedjoura et al., 2024; Stefani et al., 2024a). Operational Design Domains intend to represent the real-world conditions under which an automated, and by extension AI-based, system is intended to function (The British Standards Institution, 2020; SAE International, 2021; ISO, 2023; European Union Aviation Safety Agency (EASA), 2024). Originating from the automotive domain, the ODD is loosely defined as the specific conditions, such as environmental, geographic, and time-of-day restrictions, under which an autonomous driving system is expected to function (SAE International, 2021; ISO, 2023). The EASA definition is similar, extending it to any AI-based system and, by extension, to any AI/ML constituent (European Union Aviation Safety Agency (EASA), 2024). Moreover, the ODD is split into two parts, the taxonomy and the ontology (The British Standards Institution, 2020; Trypuz et al., 2024). The taxonomy describes the overall set of parameters and their applicable ranges, e.g., the car’s current speed or the aircraft’s altitude. The ontology,

however, describes the interrelations among those parameters and how certain parameters influence one another. An example here might be the minimum possible turning radius of a car, depending on its speed, or the landing speed of an aircraft, depending on current weather and visibility. As such, the ODD plays a critical role in Safety-by-Design AI Engineering methodologies to ensure compliance with applicable standards and regulations. However, creating the ODD is not trivial. While the ranges of some parameters can be quite evident, others, especially their interconnections, are almost impossible to define beforehand, for example, if they depend on complex processes like weather.

This clear commitment to ODDs as a standardized framework for describing operational conditions requires a comprehensive representation used not only for modeling and information exchange but also for monitors that can detect whether the system still operates within the ODD. Although some ODD representations use a structured data format like tabular representations or the YAML-based format used by ASAMs OpenODD format (Verein zur Förderung der internationalen Standardisierung von Automatisierungs- und Meßsystemen (ASAM) e.V., 2025; Werner et al., 2025), extensive mathematical representations of ODDs are still a subject of ongoing research. Most works represent the ODD as an  $n$ -dimensional space, with different approaches to constraining it. Some use convex polytopes, which provide a clean representation but cannot model more complex ODD taxonomies (Nenchev, 2025), thereby disregarding the ontology. Others provide an extensive framework for describing the ODD in great detail, but the ontology representation cannot handle constraints imposed by the parameter combination (Shakeri, 2024). Research has also been conducted to split the ODD into so-called  $\mu$ ODDs, which are used to improve handling and cover potentially complex ODDs (Koopman et al., 2019; Salvi et al., 2022). Thus, while ODDs can contain abstract definitions of the environment, they are, in general, currently defined by a parameter space that describes the overall taxonomy.

From the ODD, scenarios can be derived that provide a high-level description of operating conditions defined through a subset of parameter ranges. For example, the scenarios driving and flying at night in rainy weather would define the time-of-day to be between 6 p.m. and 6 a.m. and the precipitation and cloud coverage to be greater than zero. Sometimes, this is further split into logical and concrete scenarios, where logical scenarios define the aforementioned ranges, while concrete scenarios specify initial values for each parameter. Nevertheless, a scenario is always a series of snapshots, called scenes. Each scene is therefore a unique set of ODD parameter values, together with data from all sensors, given the current environmental conditions.

### 3. Mathematical Representation of ODDs

As previously described, multiple frameworks exist for structuring the ODD. However, all those representations lack a comprehensive yet generic framework for representing the ontology, as well as a means to compare two ODDs and determine whether they express the same problem. Both are solved with the following mathematical representation of an ODD.

Let the ODD be defined as the structure  $(X, \mathcal{R})$ , where  $X \subseteq \mathbb{R}^n$  is the parameter space, also called taxonomy, and  $\mathcal{R} = \{R_1, R_2, \dots, R_r\}$  is the set of relationships between any set of parameters, also called ontology. Then, a logical scenario can be defined as the structure  $(L, \emptyset)$ , where  $L \subseteq X$ . A concrete scenario can now be defined through any initial state vector  $x \in L$ , also called a scene. Given the state vector  $x$ ,  $R_i$  can be defined as

$$R_i(x) = \begin{cases} 1 & \text{if condition } R_i \text{ is met,} \\ 0 & \text{otherwise} \end{cases} . \quad (1)$$

Similarly,  $\mathcal{R}(x)$  is 1 if all  $R_i$  are 1 and 0 otherwise. Furthermore, let  $Y \subseteq \mathbb{R}^m$  be the data space and  $y$  be the collected data from the scene  $x$ . Thus, ideally,  $f : X \rightarrow Y$  is the mapping from the ODD parameter space  $X$  to the data space  $Y$ . However, in reality, stochastic processes influence the collected data, whether through system randomness or sensor noise, leading to  $f : X \times \Omega \rightarrow Y$ , where  $\omega \in \Omega$  denotes the system noise. By definition,  $Y$  contains only data that has been collected while operating inside the ODD; therefore,  $f$  is surjective.

**Definition 3.1** (Equality of ODD Structures). Two ODD structures  $(X_1, \mathcal{R}_1)$  and  $(X_2, \mathcal{R}_2)$  are considered equal if they generate the same data set  $Y$ .

$$\begin{aligned} \forall y \in Y, \\ \exists (x_1, \omega_1) \in X_1 \times \Omega_1, \mathcal{R}_1(x_1) = 1, y = f_1(x_1, \omega_1) \\ \iff \\ \exists (x_2, \omega_2) \in X_2 \times \Omega_2, \mathcal{R}_2(x_2) = 1, y = f_2(x_2, \omega_2) \end{aligned} \quad (2)$$

This notion of equality is data-centric and intentionally abstracts away semantic differences that cannot be resolved from observations alone.

As an example, given the definition of equality, let two ODDs be defined as  $(X_1, \mathcal{R}_1) = (\{x | x \in \mathbb{R}^2 \text{ and } 0 \leq x_1 \leq 1 \text{ and } 0 \leq x_2 \leq 1\}, \emptyset)$  with  $f_1(x, \omega) = x_1 - x_2$  and  $(X_2, \mathcal{R}_2) = (\{x | x \in \mathbb{R} \text{ and } -1 \leq x \leq 1\}, \emptyset)$  with  $f_2(x, \omega) = x$ . Thus,  $Y_1 = [-1, 1] = Y_2$ , and therefore,  $(X_1, \mathcal{R}_1) = (X_2, \mathcal{R}_2)$ . Moreover, while  $f_2 : X \times \Omega \rightarrow Y$  is injective and thus bijective,  $f_1 : X \times \Omega \rightarrow Y$  is not.

#### 3.1. High Dimensional ODD Representation

To model the ODD structure  $(X, \mathcal{R})$ , especially in higher dimensions, a robust framework is required. To model the parameter space  $X$ , polytopes have proven effective (Nenchev, 2025). In general, given the complexity of the real world, the ODD polytope is not convex. While polytopes can be concave, modeling the ODD polytope as a union of convex polytopes is helpful, enabling the use of convex optimization tools. Thus, the ODD polytope  $\mathcal{P}$  can be defined as the union of a set of  $j$  unique convex non-intersecting polytopes  $\mathcal{C}_j$  as

$$\mathcal{P} = \bigcup_{j=1}^J \mathcal{C}_j \quad (3)$$

with the half-space definition of  $\mathcal{C}$  using the component-wise inequality

$$\mathcal{C} = \{x \in \mathbb{R}^n : Ax \leq b\}, \quad (4)$$

where  $A$  is the matrix containing the normal vectors to the  $i$ -th hyperplane defining the half-space and  $b$  the right-hand side vector that determines the distance of the hyperplane from the origin.

### 4. The Kernel-Based Representation

Although the aforementioned polytope-based approach to modeling ODDs works for expert-generated ODDs with continuous parameter ranges, it is unsuitable for data-driven ODD development. However, using the concept of anchor points—the points used to derive the data-driven ODD (cf. Theorem 4.1)—, a data-driven ODD can be derived around them. While a straightforward approach is to construct the convex hull of all anchor points, this may include regions outside the ODD. Assuming the ODD is roughly described as a 2D parameter space and all anchor points fall onto a second-order polynomial, a convex hull would include the area between the polynomial, which isn't actually part of the ODD. Instead of defining  $X$  as the minimum and maximum of the parameters and deriving complex relationships  $R_i$  from the data, a data-first approach should be devised. This approach aims to identify local dependencies directly from the data, without expert knowledge. Moreover, to ensure Safety-by-Design, the order of samples must not influence the resulting ODD representation. Otherwise, this would introduce an additional source of uncertainty that should be avoided. Therefore, algorithms that enable *re-training*, such as Neural Network-based representations, cannot reliably produce a safe ODD representation. Therefore, the following section introduces a kernel-based concept to uniquely and deterministically derive an ODD from data. Given its uniqueness and determinism, this concept is the first step toward certifying AI-based systems using data-driven ODDs.

Moreover, the concept applies to both minuscule and vast amounts of data, thereby expanding the potential applications of the data-driven ODD.

#### 4.1. Formal Definition of the Kernel-Based ODD

The following subsection introduces a formal definition, followed by parameterization and algorithmic construction, to clearly separate the mathematical representation of the ODD from its data-driven instantiation. Let  $X \subseteq \mathbb{R}^n$  denote the parameter space of the Operational Design Domain (ODD), where each point  $\mathbf{x} \in X$  represents a concrete operational condition described by  $n$  continuous parameters (cf. Section 3).

**Definition 4.1** (Samples and Anchor Points). Let

$$\mathcal{D} = \mathcal{D}_{\text{ID}} \cup \mathcal{D}_{\text{OOD}} \subseteq X \quad (5)$$

be a finite dataset, where  $\mathcal{D}_{\text{ID}} \subseteq X$  denotes the set of in-distribution (ID) samples that are considered part of the ODD, and  $\mathcal{D}_{\text{OOD}} \subset X$  denotes the set of out-of-distribution (OOD) samples that are explicitly not part of the ODD. The set of anchor points

$$\mathcal{A} \subseteq \mathcal{D}_{\text{ID}} \quad (6)$$

is the finite (sub)set of samples used to parameterize the kernel-based ODD representation. In general, all ID samples are used as anchor points, i.e.,  $\mathcal{A} \equiv \mathcal{D}_{\text{ID}}$ .

**Definition 4.2** (Local Affinity Function). For each of the  $i$  anchor points  $\mathbf{x}_i \in \mathcal{A}$ , a local affinity function  $\alpha_i : X \rightarrow [0, 1]$  is defined using a positive-definite kernel.

**Definition 4.3** (Global ODD Affinity Function). The kernel-based ODD representation is defined as a global affinity function  $\alpha : X \rightarrow [0, 1]$  constructed by superposition of all local affinity functions:

$$\alpha(\mathbf{x}) = 1 - \prod_i (1 - \alpha_i(\mathbf{x})). \quad (7)$$

The value  $\alpha(\mathbf{x})$  represents the degree to which the operational condition  $\mathbf{x}$  belongs to the ODD.

**Definition 4.4** (Threshold-Based ODD Membership). Given the global affinity function  $\alpha$ , let  $\zeta \in [0, 1]$  be a predefined affinity threshold. A sample  $\mathbf{x} \in X$  is considered to be *inside* the data-driven ODD if and only if

$$\alpha(\mathbf{x}) \geq \zeta. \quad (8)$$

**Definition 4.5** (OOD Consistency Constraint). Let  $\xi \in [0, 1]$  denote a predefined maximum allowed affinity threshold for OOD samples. The kernel-based ODD representation shall satisfy

$$\alpha(\mathbf{x}) \leq \xi \quad \forall \mathbf{x} \in \mathcal{D}_{\text{OOD}}. \quad (9)$$

If this constraint is violated, the most contributing kernels must be adjusted, while keeping the anchor points fixed, until the constraint is satisfied.

**Definition 4.6** (Kernel-Based Operational Design Domain). A kernel-based Operational Design Domain is defined as the tuple

$$\mathcal{O} = (\alpha, \zeta), \quad (10)$$

where the global affinity function  $\alpha$  is deterministic, continuous over  $X$ , and bounded in  $[0, 1]$ .

#### 4.2. Choice of Kernel

For the defined affinity function (cf. Theorem 4.2 and 4.3), additional requirements can be defined. First, it shall be continuous over  $X \subseteq \mathbb{R}^n$ ; otherwise, the affinity value might not be defined for some samples. Next, the output, the affinity, shall be bounded to  $[0, 1]$  and approach 0 for  $|\mathbf{x} - \mathbf{x}_i| \rightarrow \infty$ . As ODDs can have an unlimited number of parameters, thus an unlimited number of dimensions, the affinity function itself shall be expandable to infinitely many dimensions. Finally, although not strictly required, a parameterizable, computationally efficient affinity function is helpful, enabling easy adaptation to specific use cases and requirements and facilitating online use of the derived affinity function representing the data-driven ODD. All these requirements point to kernels as the best approach for approximating the affinity function. They are generally continuous, approach 0 for extreme inputs, can adapt to a large number of dimensions, and can be tuned using their respective parameter matrices. Moreover, they are well-studied, making them the perfect candidates. Some possible kernels are the Laplacian kernel (Rupp, 2015), the leptokurtic Cauchy-Lorentz kernel (Feller, 2009), cubic spline kernel (Monaghan, 1992), and finally the radial-basis function (RBF) kernel (Hastie et al., 2009). This work focuses on the RBF kernel, which can be defined as

$$\alpha_i(\mathbf{x}) = \exp \left( -\frac{1}{2} (\mathbf{x} - \mathbf{x}_i)^\top \Sigma_i^{-1} (\mathbf{x} - \mathbf{x}_i) \right) \quad (11)$$

for multi-dimensional systems, where  $\alpha_i$  is the kernel function, i.e., affinity function, for the  $i$ -th anchor point,  $\mathbf{x}_i \in \mathbb{R}^n$  is the  $i$ -th anchor point itself, and  $\Sigma_i \in \mathbb{R}^{n \times n}$  is the symmetric, positive-definite free parameter matrix associated with the  $i$ -th anchor point  $\mathbf{x}_i$ .

Given that an ODD is derived from multiple anchor points, each with its own unique kernels and thus affinity functions, a superposition is required to obtain a global affinity value for any given sample. The superposition function, see Theorem 4.3, must also be bounded to  $[0, 1]$ , just like the affinity function for each anchor point. Therefore, when multiple anchor points are at the same location, their respective affinities cannot be additive; they must be multiplicative. From here follows the superposition, and thus the global affinity function, as defined in Equation (7).

### 4.3. Choosing the Kernel Parameters

Almost every kernel has a free parameter matrix. Defining all those parameters by hand would undermine the purpose of an automated, data-driven ODD derivation framework. Moreover, for the RBF kernel,  $N$  n-dimensional anchor points would lead to up to  $Nn^2$  parameters to define. To allow automated parameter definition, some assumptions and simplifications must be made. First, it is assumed that the parameters are locally independent and relationships are governed only by global effects. From this simplification, it follows that the  $\Sigma$  matrix is diagonal. Moreover, it can be assumed that areas with a higher density of anchor points are more likely to be part of the ODD rather than outliers. Thus, the corresponding parameter in the  $\Sigma$  matrix may be larger, resulting in a wider influence of the kernel. Therefore, the parameters depend only on the distance to the nearest neighbor. With this assumption, the entries of the  $\Sigma$  matrix can be defined as

$$\sigma_{kk}^{(i)} = \kappa \exp(-\eta d_i^*), \quad k = 1, \dots, n, \quad (12)$$

where  $\sigma_{kk}^{(i)}$  are the diagonal entries of the  $\Sigma$  matrix for the RBF kernel of the  $i$ -th anchor point,  $\kappa$  is the maximum value of the diagonal entry,  $\eta$  is the decay factor and  $d_i^*$  is the distance to the nearest neighbor, either globally or per dimension. This approach reduces the number of manually defined parameters from  $Nn^2$  to 2, or 2n if  $\kappa$  and  $\eta$  are defined per dimension.

This, however, can lead to unstable matrix entries when anchor points are spread far apart, as the corresponding  $\sigma_{kk}^{(i)}$  will be rather small and in turn the corresponding entries in  $\Sigma^{-1}$  can become numerically unstable. Here, two alternatives are sensible. The first, and more generic, approach is to define a lower limit for Equation (12). This would lead to a function similar to

$$\sigma_{kk}^{(i)} = (\kappa - \lambda) \exp(-\eta d_i^*) + \lambda, \quad k = 1, \dots, n, \quad (13)$$

where  $\lambda$  is the lower bound of  $\sigma_{kk}^{(i)}$ . The second approach would be to normalize the parameter ranges. This approach would ensure that all ranges are again in the same order of magnitude and thus their corresponding diagonal matrix entries are also roughly in the same order of magnitude, reducing the likelihood of extreme matrix entries making the affinity function unstable.

### 4.4. Handling Out-of-Distribution Data

Often, the data used to define the data-driven ODD not only includes in-distribution (ID) samples as anchor points, but also out-of-distribution (OOD) samples explicitly outside the ODD. Here, it is important to ensure that these points are not later classified as part of the ODD. However, most kernels, especially the RBF kernel, cannot be zero anywhere;

instead, a maximum affinity score can be defined at the locations of OOD samples. Inspired by the Development Assurance Levels (SAE International, 2023), depending on the classification of failure conditions of the AI-based systems, different maximum values can be defined. After calculating the kernel parameters purely on ID samples, the global affinity function  $\alpha(\mathbf{x})$  has to be sampled at all OOD sample locations. If the affinity is above the defined threshold, the most influential kernels have to be tuned such that  $\alpha(\mathbf{x})$  stays below the threshold.

### 4.5. Creation of the Kernel-Based ODD

All previously mentioned steps are combined in Algorithm 1, which defines how to derive the ODD from data. First, the available data has to be collected and split into ID and OOD samples. Next, a kernel must be chosen and their corresponding tuning parameters, similar to Equation (12) must be defined, see Section 4.3. Then, for each anchor point, the nearest neighbors of the ID samples must be found, either globally or per dimension. Based on the nearest neighbors, or more precisely, the distance to them, the kernel for every anchor point can be defined. Finally, if they exist, the affinity of every OOD sample must be checked to ensure it is below the defined limit.

---

#### Algorithm 1 Automated Kernel-Based ODD Derivation

---

```

1: Input:
2:   Dataset  $\mathcal{D} = \mathcal{D}_{\text{ID}} \cup \mathcal{D}_{\text{OOD}}$ 
3:   Kernel type (e.g., RBF)
4:   Kernel parameters (e.g.,  $\kappa, \eta$ )
5:   OOD affinity threshold  $\xi$ 
6: Anchor Point Selection:
7:   Set anchor points  $\mathcal{A} \leftarrow \mathcal{D}_{\text{ID}}$ 
8: Kernel Parameter Estimation:
9:   for each anchor point  $\mathbf{x}_i \in \mathcal{A}$  do
10:    Compute distance  $d_i^*$  to the nearest neighboring anchor point
11:    for each dimension  $k$  do
12:      Set  $\sigma_{kk}^{(i)} \leftarrow (\kappa - \lambda) \exp(-\eta d_i^*) + \lambda$ 
13:    end for
14:    Define kernel  $\alpha_i(\mathbf{x})$  using  $\Sigma_i$ 
15:  end for
16: OOD Consistency Check (cf. Theorem 4.5):
17:  for each  $\mathbf{x}_{\text{OOD}} \in \mathcal{D}_{\text{OOD}}$  do
18:    if  $\alpha(\mathbf{x}_{\text{OOD}}) > \xi$  then
19:      Identify dominant kernels contributing to  $\alpha(\mathbf{x}_{\text{OOD}})$ 
20:      Adjust corresponding  $\Sigma_i$  to reduce affinity
21:    end if
22:  end for
23: Output: Deterministic kernel-based ODD affinity function  $\alpha(\mathbf{x})$ 

```

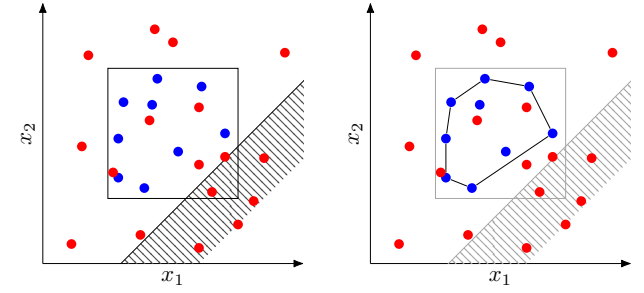
---

## 5. Validation

To validate the method of deriving the ODD  $\mathcal{O}$  from data, a tool called autoSAFE has been developed and open-sourced<sup>1</sup>. The Python-based tool provides a sophisticated interface for various applications, including Monte Carlo-based sampling for validation (cf. subsection 5.1) and the provision of real-world data in different formats (cf. subsection 5.2). The tool can parse data from a wide range of sources, including CSV files, NumPy-like arrays, dataframes, and, most importantly, the JSON-based ASAM OpenLABEL format (Verein zur Förderung der internationalen Standardisierung von Automatisierungs- und Meßsystemen (ASAM) e.V., 2021). The latter is an annotation format commonly used in the automotive domain, designed to facilitate the labeling and tracking of objects across multiple scenes. The data is then converted into an internal kernel-based representation that enables fast, efficient querying of the affinity value for one or more sample points. Thus, it can be integrated into current development methodologies and used as an online tool to determine whether new, unseen samples fall within the ODD, thereby enhancing the safety of already deployed AI-based systems. This is achieved using a set of libraries, such as NumPy (Harris et al., 2020) and SciPy (Virtanen et al., 2020) for efficient data handling, polytope (Filippidis et al., 2016) for representing ODD polytopes (cf. Section 3), and Faiss (Johnson et al., 2021; Douze et al., 2025) for fast nearest-neighbor searches.

### 5.1. Monte-Carlo Method

Monte Carlo methods (MCM) (Metropolis & Ulam, 1949) have proven useful for numerical problem solving. Instead of analytically solving a problem, repeated stochastic processes can approximate a wide variety of problems, from approximating  $\pi$  to simulating elementary particles or developing new materials (Kroese et al., 2014). Here, MCM can be used to simulate high-dimensional ODDs by randomly distributing anchor points and generating validation samples in equal proportions, thereby enabling the determination of ODD affiliation and affinity values. To validate the method presented in this work, first, a random ODD structure  $(X, \mathcal{R})$  is generated. Here,  $X$  is a multi-dimensional hyperrectangle, and  $\mathcal{R}$  a set of polynomial inequalities. A simple 2D case is depicted in Figure 1a, where the blue dots are the anchor points, the red dots are the validation samples, the black rectangle is the polytope  $X$ , and the black line is the relationship  $R_1$ , a single linear inequality. For this setup, the data-driven ODD  $\mathcal{O}$  has been derived according to Algorithm 1 with varying numbers of anchor points to validate the method not only for a large amount of available anchor points but also for the minimum possible amount.



(a) Setup for comparing the data-driven ODD  $\mathcal{O}$  to the underlying original ODD. The black rectangle represents the polytope  $X$  and the black line depicts the inequality  $R_1$ .

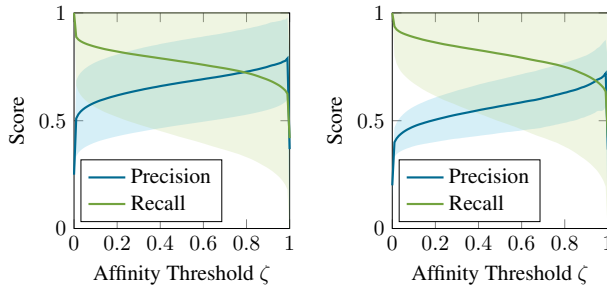
(b) Setup for comparing the data-driven ODD  $\mathcal{O}$  to the convex hull of all anchor points.

Figure 1. Setup for the 2D example of the Monte-Carlo method. The blue dots are the anchor points from which the data-driven ODD  $\mathcal{O}$  is derived. The red dots are the validation samples to compare the data-driven ODD  $\mathcal{O}$  to the underlying original ODD.

More precisely,  $X$  was defined as  $[-5, 5] \times [-5, 5]$ ,  $R_1$  as  $x_2 \geq x_1 - 3$  and the number of anchor points was varied from 3 up to 10 000. Each number of anchor points was validated against 100 000 validation samples to ensure sufficient validation points are close to the anchor points and within the ODD. Their range was set to be double that of  $X$ , meaning they were sampled in the  $[-10, 10] \times [-10, 10]$  hyperrectangle. Next, for all validation points and all anchor point configurations, the affinity and whether each point lies within the original ODD were calculated. Based on the data, the confusion matrix was computed for different affinity thresholds. Here, the affinity threshold determines whether a validation sample point is classified as inside the data-driven ODD. Validation samples with affinity values at or above the affinity threshold  $\zeta$  are considered within the data-driven ODD; those below it are not. Given the results, a precision recall plot was created (cf. Figure 2a). The precision-recall curves are averages across all numbers of anchor points. Generally speaking, increasing the number of anchor points decreases precision while increasing recall. The shaded area is the standard deviation of the data. Moreover, the sharp edges where the affinity is either zero or one can be explained by the fact that the used RBF kernel cannot be exactly zero; it can only be close to zero, so there are no validation samples with exactly zero affinity. Similarly, for the validation samples to have an affinity precisely equal to 1, they would have to land exactly on an anchor point. Given the precision-recall plots, one can derive an affinity threshold for the use case by balancing precision and recall to achieve the optimal balance within overall constraints, such as required safety levels. However, the data-driven approach was adopted because the underlying ODD is unavailable. Thus, to accurately validate the data-driven ODD  $\mathcal{O}$ , it cannot be compared just to the known ODD, as it

<sup>1</sup><https://github.com/DLR-KI/autosafe>

will not be available in a real-world application. Instead, to validate the approach, the data-driven ODD  $\mathcal{O}$  is also validated against a convex hull of all the anchor points as it comes closest to the underlying ODD structure  $(X, \mathcal{R})$ . This approach is illustrated in Figure 1b, where the original ODD structure is still drawn, albeit faintly. The same steps as before were repeated, and a corresponding precision recall plot was created (cf. Figure 2b). Comparing the two approaches reveals a clear similarity, further underscored by the coefficient of determination ( $R^2$ ) between the precision-recall curves of the original ODD and the convex hull. More precisely, for the precision  $R^2 = 0.9855$  and for the recall  $R^2 = 0.9987$ . From these numbers, it is clear that the general method works. Similar results have been achieved for the MCM approach with up to 10 dimensions and more complex relationship functions. For all conducted tests, the coefficients of determination were above 0.973.



(a) Precision-recall curves when comparing the data-driven ODD to the original underlying ODD. (b) Precision-recall curves when comparing the data-driven ODD to the convex hull of all anchor points.

Figure 2. Precision-recall curves for a data-driven ODD where the underlying ODD is defined as  $(X = [-5, 5] \times [-5, 5], \mathcal{R} = \{R_1 : x_2 \geq x_1 - 3\})$  (cf. Figure 1). The results show that similar precision-recall curves can be derived from the convex hull compared to the original underlying ODD.

## 5.2. Real World Use Case

In aviation, one of the most important tasks of pilots during en route travel is avoiding collisions with other aircraft. The next generation of collision avoidance systems is expected to significantly improve performance; however, it has become apparent that the proposed system cannot run on current state-of-the-art avionics hardware because its memory requirements are too high (Damour et al., 2021). This prompted diverse research, leading to the development of VCAS, a minimal reimplemention of the system that uses neural networks for policy compression (Julian et al., 2016). Thus, a stringed safety argumentation will be required for an AI-based collision-avoidance system (Christensen et al., 2024b). Given that the standards clearly define the operational conditions, an appropriate ODD can be derived and later compared with the ODD derived by autoSAFE. There-

fore, this use case is a prime example for further study in this work. However, in line with previous research (Julian & Kochenderfer, 2019), only a subset of the full operational conditions will be examined. For VCAS, the decision depends on the relative altitude between the ownship and the intruder, their corresponding vertical rates, the time to closest point of approach (CPA), and the advisory issued in the previous time step. A geometric overview of this problem is given in Figure 3. Furthermore, the parameter ranges are

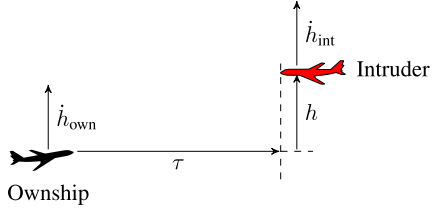


Figure 3. Geometry of the vertical collision avoidance scenario for VCAS, from (Julian & Kochenderfer, 2019). The black ownship is trying to avoid the (malicious) red intruder by diverting through climbing or descending.

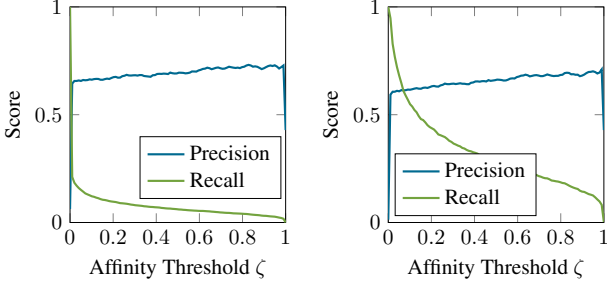
shown in Table 1. Based on these parameter ranges and

Table 1. Parameter ranges for the taxonomy  $X$  in the VCAS use case. The ranges are a subset of the original VCAS implementation (Julian & Kochenderfer, 2019).

| Variable         | Description         | Range   |
|------------------|---------------------|---|
| $h$              | Relative altitude   | [-1500 m, 1500 m]                               |
| $h_{\text{own}}$ | Ownship vert. rate  | [-26 m s <sup>-1</sup> , 26 m s <sup>-1</sup> ] |
| $h_{\text{int}}$ | Intruder vert. rate | 0 m s <sup>-1</sup>                             |
| $\tau$           | Time to CPA         | [0 s, 40 s]                                     |
| $s_{\text{adv}}$ | Previous advisory   | [0, 1, 2, ..., 8]                               |

previous experiments from other works (Christensen et al., 2024a; Stefani et al., 2024b), a dataset of all observed state vectors has been created. In total, this included 622 110 anchor points. Next, they were used to create the data-driven ODD  $\mathcal{O}$  using the RBF kernel. Additionally, the convex hull was created. Once the data-driven ODD  $\mathcal{O}$  had been created,  $10^7$  validation samples in and around the parameter ranges defined in Table 1 were created. As before, for each validation sample, the affinity value and its membership in the underlying ODD and the convex hull were calculated. Subsequently, the confusion matrix was computed for different affinity thresholds, and precision-recall plots were generated. The resulting plots are shown in Figure 4. In general, the curves follow a trend similar to the MCM results, indicating that the data-driven ODD approach performs well in a real-world use case. The generally lower and steeper recall curves can be explained by the lower density of anchor points within the 5D hyperrectangle compared to the MCM example. Thus, the overall recall is smaller, as more

false negative validation samples—samples that are inside the underlying ODD but are not classified as such by the data-driven ODD  $\mathcal{O}$ —exist. Again, the coefficients of determination between the underlying ODD and the convex hull were calculated to be  $R^2 = 0.991\,05$  for the precision and  $R^2 = 0.999\,79$  for the recall, respectively. This again suggests that the convex hull is an adequate approximation to define the affinity threshold based on precision and recall.



(a) Precision-recall curves when comparing the data-driven ODD to the original underlying ODD (left) and the convex hull over all anchor points (right) is noticeable, confirming the data-driven ODD approach.

Figure 4. Resulting precision-recall curves for the VCAS use case. Again, a strong similarity between the underlying original ODD (left) and the convex hull over all anchor points (right) is noticeable, confirming the data-driven ODD approach.

## 6. Discussion

The results presented in Section 5 demonstrate that the proposed kernel-based approach can effectively approximate an underlying ODD solely from data. This capability is crucial for legacy systems or complex environments where an analytic description of the ODD is unavailable or incomplete. A key finding is the high coefficient of determination between the performance of the data-driven ODD and the convex hull of the anchor points. This correlation suggests that, even without access to the ground-truth ODD, the convex hull can serve as a reliable proxy for tuning the affinity thresholds—the precision-recall trade-off—during the validation phase.

However, it is imperative to distinguish the role of the convex hull as a validation proxy from its suitability as a final ODD representation. While useful for checking coverage metrics, a convex hull is generally inadequate for the actual certification and operation of safety-critical systems. Real-world operational parameters often form non-convex, manifold-like structures with *holes* or concavities (e.g., specific combinations of altitude and speed that are physically impossible or unsafe). A convex hull blindly encloses these void regions, potentially deeming the system safe in conditions where no data exist and safety cannot be verified. In

contrast, the proposed kernel-based method tightly wraps around the data manifold, naturally excluding non-convex void regions and adhering to the Safety-by-Design principle of conservatism.

Furthermore, the continuous nature of the affinity function  $\alpha(\mathbf{x})$  introduces a built-in mechanism for outlier detection and runtime monitoring. Unlike rigid geometric boundaries that provide a binary inside/outside classification, the affinity score offers a measure of proximity to known safe conditions. As the system state drifts away from the anchor points,  $\alpha(\mathbf{x})$  decays smoothly. This property enables the definition of graded warning zones, allowing the system to trigger degradation modes or alert operators before the hard safety boundary is crossed. This *soft* boundary is a distinct advantage of the kernel-based representation over traditional Boolean logic ODD definitions.

## 7. Conclusion

This work showed that, although a fully truthful data-driven reconstruction of an Operational Design Domain (ODD) is not always possible, the proposed approach can sufficiently approximate the underlying ODD. Importantly, the presented method ensures that the resulting ODD is deterministic, order-independent, and conservative, satisfying key Safety-by-Design requirements for certification. By using a kernel-based representation, the framework provides a mathematically rigorous means to define operational boundaries that are interpretable and tractable.

Future work will focus on optimizing the kernel hyperparameter selection process. While this work focused on diagonal kernel parameter matrices to enhance robustness and interpretability, selectively extending the framework to model cross-dimensional dependencies could further improve expressiveness in tightly coupled systems. Such extensions would require careful constraints to preserve determinism and certifiability. Moreover, integrating temporal information represents a promising extension. Many operational constraints are inherently dynamic, and incorporating time-dependent kernels could enable the representation of evolving or context-dependent ODDs. This would be particularly relevant for systems operating in highly dynamic environments, such as air traffic management or autonomous driving. Finally, future work should explore tighter integration of kernel-based ODDs into certification workflows. This includes linking affinity thresholds to formal safety requirements, leveraging the representation for runtime assurance monitors, and studying how data-driven ODD updates can be performed in a controlled and certifiable manner. Such developments would further strengthen the role of data-driven ODDs as a practical tool for deploying safety-critical AI-based systems.

## Impact Statement

This paper presents work whose goal is to advance the field of Machine Learning. There are many potential societal consequences of our work, none which we feel must be specifically highlighted here.

## References

Adedjouma, M., Botella, B., Ibanez-Guzman, J., Mantissa, K., Proum, C.-M., and Smaoui, A. Defining operational design domain for autonomous systems: A domain-agnostic and risk-based approach. In *SOSE 2024 - 19th Annual System of Systems Engineering Conference*, pp. 166–171, Tacoma, WA, United States, 06 2024. IEEE. doi: 10.1109/SOSE62659.2024.10620936.

Bello, H., Geißler, D., Ray, L., Müller-Divéky, S., Müller, P., Kittrell, S., Liu, M., Zhou, B., and Lukowicz, P. Towards certifiable ai in aviation: landscape, challenges, and opportunities. 2024.

Christensen, J. M., Anilkumar Girija, A., Stefani, T., Durak, U., Hoemann, E., Köster, F., Krüger, T., and Hallerbach, S. Advancing the ai-based realization of acas x towards real-world application. In *2024 IEEE 36th International Conference on Tools with Artificial Intelligence (ICTAI)*, pp. 57–64, Herndon, VA, USA, 10 2024a. IEEE. ISBN 979-8-3315-2723-5. doi: 10.1109/ICTAI62512.2024.00017.

Christensen, J. M., Zaeske, W., Beck, J., Friedrich, S., Stefani, T., Girija, A. A., Hoemann, E., Durak, U., Köster, F., Krüger, T., and Hallerbach, S. Towards certifiable ai in aviation: A framework for neural network assurance using advanced visualization and safety nets. In *2024 AIAA DATC/IEEE 43rd Digital Avionics Systems Conference (DASC)*, pp. 1–9, San Diego, CA, USA, 09 2024b. IEEE. ISBN 979-8-3503-4961-0. doi: 10.1109/dasc62030.2024.10749321.

Christensen, J. M., Stefani, T., Anilkumar Girija, A., Hoemann, E., Vogt, A., Werbilo, V., Durak, U., Köster, F., Krüger, T., and Hallerbach, S. Formulating an engineering framework for future ai certification in aviation. *Aerospace*, 12(6):1–27, 05 2025. ISSN 2226-4310. doi: 10.3390/aerospace12060482. URL <https://www.mdpi.com/2226-4310/12/6/482>.

Damour, M., De Grancey, F., Gabreau, C., Gaufffria, A., Ginestet, J.-B., Hervieu, A., Huriaux, T., Pagetti, C., Ponsonne, L., and Clavière, A. Towards certification of a reduced footprint acas-xu system: A hybrid ml-based solution. In *Computer Safety, Reliability, and Security*, pp. 34–48, Cham, Switzerland, 2021. Springer International Publishing. ISBN 978-3-030-83903-1. doi: 10.1007/978-3-030-83903-1\_3.

Douze, M., Guzhva, A., Deng, C., Johnson, J., Szilvassy, G., Mazaré, P.-E., Lomeli, M., Hosseini, L., and Jégou, H. The faiss library. *IEEE Transactions on Big Data*, pp. 1–17, 10 2025. ISSN 2332-7790. doi: 10.1109/TBDA.2025.3618474.

European Union Aviation Safety Agency (EASA). Easa concept paper: Guidance for level 1 & 2 machine learning applications. techreport, European Union Aviation Safety Agency (EASA), Postfach 10 12 53, 50452 Cologne, Germany, 04 2024. URL <https://www.easa.europa.eu/en/document-library/general-publications/easa-artificial-intelligence-concept-paper-issue-2>.

Feller, W. *An Introduction to Probability Theory and Its Applications*, volume 2 of Wiley series in probability and mathematical statistics. Wiley, [S.l.], 2 edition, 01 2009. ISBN 9780471257097. Literaturverz. S. 655 - 656.

Filippidis, I., Dathathri, S., Livingston, S. C., Ozay, N., and Murray, R. M. Control design for hybrid systems with tulip: The temporal logic planning toolbox. In *2016 IEEE Conference on Control Applications (CCA)*, pp. 1030–1041. IEEE, 09 2016. doi: 10.1109/cca.2016.7587949.

Harris, C. R., Millman, K. J., van der Walt, S. J., Gommers, R., Virtanen, P., Cournapeau, D., Wieser, E., Taylor, J., Berg, S., Smith, N. J., Kern, R., Picus, M., Hoyer, S., van Kerkwijk, M. H., Brett, M., Haldane, A., del Río, J. F., Wiebe, M., Peterson, P., Gérard-Marchant, P., Sheppard, K., Reddy, T., Weckesser, W., Abbasi, H., Gohlke, C., and Oliphant, T. E. Array programming with numpy. *Nature*, 585(7825):357–362, 09 2020. ISSN 1476-4687. doi: 10.1038/s41586-020-2649-2. URL <https://www.nature.com/articles/s41586-020-2649-2>.

Hastie, T., Tibshirani, R., and Friedman, J. *The Elements of Statistical Learning*. Springer Series in Statistics. Springer New York, New York, NY, second edition, 02 2009. ISBN 978-0-387-84857-0. doi: 10.1007/978-0-387-84858-7. Description based on publisher supplied metadata and other sources.

Huseynzade, S. Creation of an operational desing document for the autonomous shipping industry, 10 2023. URL <https://urn.fi/URN:NBN:fi-fe20231005138964>.

ISO. *ISO 34503: Road Vehicles – Test scenarios for automated driving systems – Specification for operational design domain*. Beuth Verlag, Berlin, Germany, 08 2023.

Johnson, J., Douze, M., and Jégou, H. Billion-scale similarity search with GPUs. *IEEE Transactions on Big*

*Data*, 7(3):535–547, 07 2021. ISSN 2332-7790. doi: 10.1109/TBDDATA.2019.2921572.

Julian, K. D. and Kochenderfer, M. J. Guaranteeing safety for neural network-based aircraft collision avoidance systems. In *2019 IEEE/AIAA 38th Digital Avionics Systems Conference (DASC)*, pp. 1–10, San Diego, CA, USA, 09 2019. IEEE. ISBN 978-1-7281-0649-6. doi: 10.1109/dasc43569.2019.9081748.

Julian, K. D., Lopez, J., Brush, J. S., Owen, M. P., and Kochenderfer, M. J. Policy compression for aircraft collision avoidance systems. In *2016 IEEE/AIAA 35th Digital Avionics Systems Conference (DASC)*, pp. 1–10, Sacramento, CA, USA, 09 2016. IEEE. ISBN 978-1-5090-2523-7. doi: 10.1109/DASC.2016.7778091.

Koopman, P., Osyk, B., and Weast, J. Autonomous vehicles meet the physical world: Rss, variability, uncertainty, and proving safety. In Romanovsky, A., Troubitsyna, E., and Bitsch, F. (eds.), *Computer Safety, Reliability, and Security*, pp. 245–253, Cham, 2019. Springer International Publishing. ISBN 978-3-030-26601-1. doi: 10.1007/978-3-030-26601-1\_17.

Kroese, D. P., Brereton, T., Taimre, T., and Botev, Z. I. Why the monte carlo method is so important today. *WIREs Computational Statistics*, 6(6):386–392, 06 2014. ISSN 1939-0068. doi: 10.1002/wics.1314.

Mamalet, F., Jenn, E., Flandin, G., Delsenay, H., Gabreau, C., Gauffriau, A., Beaudouin, B., Ponsolle, L., Alecu, L., Bonnin, H., Beltran, B., Duchel, D., Ginestet, J.-B., Hervieu, A., Pasquet, S., Delmas, K., Pagetti, C., Gabriel, J.-M., Chapdelaine, C., Picard, S., Damour, M., Cappi, C., Gardès, L., Grancey, F. D., Lefevre, B., Gerchinovitz, S., and Albore, A. White paper machine learning in certified systems. Research report, IRT Saint Exupéry ; ANITI, 03 2021. URL <https://hal.science/hal-03176080>.

Metropolis, N. and Ulam, S. The monte carlo method. *Journal of the American Statistical Association*, 44(247): 335–341, 09 1949. ISSN 1537-274X. doi: 10.1080/01621459.1949.10483310.

Monaghan, J. J. Smoothed particle hydrodynamics. *Annual Review of Astronomy and Astrophysics*, 30(1):543–574, 09 1992. ISSN 1545-4282. doi: 10.1146/annurev.aa.30.090192.002551.

Nenchev, V. One stack, diverse vehicles: Checking safe portability of automated driving software. In *2025 IEEE/SICE International Symposium on System Integration (SII)*, pp. 764–769, Munich, Germany, 01 2025. IEEE. doi: 10.1109/SII59315.2025.10870905.

Rabe, M., Milz, S., and Mader, P. Development methodologies for safety critical machine learning applications in the automotive domain: A survey. In *Proceedings of the IEEE/CVF Conference on Computer Vision and Pattern Recognition (CVPR) Workshops*, pp. 129–141, Nashville, TN, USA, 06 2021. doi: 10.1109/CVPRW53098.2021.00023.

Rupp, M. Machine learning for quantum mechanics in a nutshell. *International Journal of Quantum Chemistry*, 115(16):1058–1073, 07 2015. ISSN 1097-461X. doi: 10.1002/qua.24954.

SAE International. Taxonomy and definitions for terms related to driving automation systems for on-road motor vehicles: J3016. Technical Report J3016, SAE International, 04 2021. URL <https://www.sae.org/standards/content/j3016/>.

SAE International. Guidelines for development of civil aircraft and systems (ARP4754B). Technical Report ARP4754B, SAE International, 12 2023. URL <https://www.sae.org/standards/content/arp4754b/>.

Salvi, A., Weiss, G., Trapp, M., Oboril, F., and Buerkle, C. Fuzzy interpretation of operational design domains in autonomous driving. In *2022 IEEE Intelligent Vehicles Symposium (IV)*, pp. 1261–1267, Aachen, Germany, 06 2022. IEEE. ISBN 978-1-6654-8821-1. doi: 10.1109/IV51971.2022.9827061.

Shakeri, A. Formalization of operational domain and operational design domain for automated vehicles. In *2024 IEEE 24th International Conference on Software Quality, Reliability, and Security Companion (QRS-C)*, pp. 990–997, Cambridge, United Kingdom, 07 2024. IEEE. ISBN 979-8-3503-6565-8. doi: 10.1109/QRS-C63300.2024.00131.

Stefani, T., Anilkumar Girija, A., Mut, R., Hallerbach, S., and Krüger, T. From the concept of operations towards an operational design domain for safe ai in aviation. In *DLRK 2023*, pp. 1–8, Stuttgart, Germany, 09 2023. Deutsche Gesellschaft für Luft- und Raumfahrt - Lilienthal-Oberth e.V. URL <https://elib.dlr.de/197957/>.

Stefani, T., Christensen, J. M., Anilkumar Girija, A., Gupta, S., Durak, U., Köster, F., Krüger, T., and Hallerbach, S. Automated scenario generation from operational design domain model for testing ai-based systems in aviation. *CEAS Aeronautical Journal*, 16(1):197–212, 11 2024a. ISSN 1869-5590. doi: 10.1007/s13272-024-00772-4.

Stefani, T., Christensen, J. M., Hoemann, E., Anilkumar Girija, A., Köster, F., Krüger, T., and Hallerbach,

S. Applying model-based system engineering and devops on the implementation of an ai-based collision avoidance system. In *34th Congress of the International Council of the Aeronautical Sciences (ICAS)*, pp. 1–12, Florence, Italy, 09 2024b. CEAS. URL [https://www.icas.org/icas\\_archive/icas2024/data/preview/icas2024\\_0869.htm](https://www.icas.org/icas_archive/icas2024/data/preview/icas2024_0869.htm).

The British Standards Institution. *PAS 1883:2020 - Operational Design Domain (ODD) taxonomy for an automated driving system (ADS) – Specification*. BSI Standards Limited, 08 2020. ISBN 9780539067354. URL <https://www.bsigroup.com/en-GB/insights-and-media/insights/brochures/pas-1883-operational-design-domain-odd-taxonomy-for-ads-specification/>.

Trypuz, R., Kulicki, P., and Sopek, M. Ontology of autonomous driving based on the sae j3016 standard. *Semantic Web*, 15(5):1837–1862, 10 2024. ISSN 1570-0844. doi: 10.3233/SW-243578.

Verein zur Förderung der internationalen Standardisierung von Automatisierungs- und Meßsystemen (ASAM) e.V. Asam openlabel 1.0.0, 11 2021. URL <https://www.asam.net/standards/detail/openlabel/>.

Verein zur Förderung der internationalen Standardisierung von Automatisierungs- und Meßsystemen (ASAM) e.V. Asam openodd base standard 1.0.0 specification, 04 2025. URL [https://publications.pages.asam.net/standards/ASAM\\_OpenODD/ASAM\\_OpenODD/latest/specification/index.html](https://publications.pages.asam.net/standards/ASAM_OpenODD/ASAM_OpenODD/latest/specification/index.html).

Virтанен, P., Гоммерс, R., Олифант, T. E., Haberland, M., Reddy, T., Cournapeau, D., Буровский, E., Peterson, P., Weckesser, W., Bright, J., van der Walt, S. J., Brett, M., Wilson, J., Millman, K. J., Mayorov, N., Nelson, A. R. J., Jones, E., Kern, R., Larson, E., Carey, C. J., Polat, İ., Feng, Y., Moore, E. W., VanderPlas, J., Laxalde, D., Perktold, J., Cimrman, R., Henriksen, I., Quintero, E. A., Harris, C. R., Archibald, A. M., Ribeiro, A. H., Pedregosa, F., van Mulbregt, P., Vijaykumar, A., Bardelli, A. P., Rothberg, A., Hilboll, A., Kloeckner, A., Scopatz, A., Lee, A., Rokem, A., Woods, C. N., Fulton, C., Masson, C., Häggström, C., Fitzgerald, C., Nicholson, D. A., Hagen, D. R., Pasechnik, D. V., Olivetti, E., Martin, E., Wieser, E., Silva, F., Lenders, F., Wilhelm, F., Young, G., Price, G. A., Ingold, G.-L., Allen, G. E., Lee, G. R., Audren, H., Probst, I., Dietrich, J. P., Silterra, J., Webber, J. T., Slavić, J., Nothman, J., Buchner, J., Kulick, J., Schönberger, J. L., de Miranda Cardoso, J. V., Reimer, J., Harrington, J., Rodríguez, J. L. C., Nunez-Iglesias, J., Kuczynski, J., Tritz, K., Thoma, M., Newville, M., Kümmerer, M., Bolingbroke, M., Tartre, M., Pak, M., Smith, N. J., Nowaczyk, N., Shebanov, N., Pavlyk, O., Brodkorb, P. A., Lee, P., McGibbon, R. T., Feldbauer, R., Lewis, S., Tygier, S., Sievert, S., Vigna, S., Peterson, S., More, S., Pudlik, T., Oshima, T., Pingel, T. J., Robitaille, T. P., Spura, T., Jones, T. R., Cera, T., Leslie, T., Zito, T., Krauss, T., Upadhyay, U., Halchenko, Y. O., and Vázquez-Baeza, Y. Scipy 1.0: fundamental algorithms for scientific computing in python. *Nature Methods*, 17(3):261–272, 02 2020. ISSN 1548-7105. doi: 10.1038/s41592-019-0686-2.

Werner, F., Christensen, J. M., Stefani, T., Köster, F., Hemann, E., and Hallerbach, S. Formulating a learning assurance-based framework for ai-based systems in aviation. *Preprints*, 11 2025. doi: 10.20944/preprints202511.0786.v1.